Determining the Membrane Topology of Peptides by Fluorescence Quenching[†]

William C. Wimley[‡] and Stephen H. White*

Department of Physiology and Biophysics, University of California at Irvine, Irvine, California 92697-4560

Received August 6, 1999; Revised Manuscript Received October 26, 1999

ABSTRACT: Determination of the topology of peptides in membranes is important for characterizing and understanding the interactions of peptides with membranes. We describe a method that uses fluorescence quenching arising from resonance energy transfer ("FRET") for determining the topology of the tryptophan residues of peptides partitioned into phospholipid bilayer vesicles. This is accomplished through the use of a novel lyso-phospholipid quencher (lysoMC), N-(7-hydroxyl-4-methylcoumarin-3-acetyl)-1-palmitoyl-2-hydroxy-*sn*-glycero-3-phosphoethanolamine. The design principle was to anchor the methylcoumarin quencher in the membrane interface by attaching it to the headgroup of lyso-phosphoethanolamine. We show that lysoMC can be incorporated readily into large unilamellar phospholipid vesicles to yield either symmetrically (both leaflets) or asymmetrically (outer leaflet only) labeled bilayers. LysoMC quenches the fluorescence of membrane-bound tryptophan by the Förster mechanism with an apparent R_0 that is comparable to the thickness of the hydrocarbon core of a lipid bilayer (~25 Å). Consequently, the methylcoumarin acceptor predominantly quenches tryptophans that reside in the same monolayer as the probe. The topology of a peptide's tryptophan in membranes can be determined by comparing the quenching in symmetric and asymmetric lysoMC-labeled vesicles. Because it is essential to know that asymmetrically incorporated lysoMC remains so under all conditions, we also developed a second type of FRET experiment for assessing the rate of transbilayer diffusion (flip-flop) of lysoMC. Except in the presence of pore-forming peptides, there was no measurable flip-flop of lysoMC, indicating that asymmetric distributions of quencher are stable. We used these methods to show that *N*-acetyl-tryptophan-octylamide and tryptophan-octylester rapidly equilibrate across phosphatidylcholine (POPC) and phosphatidylglycerol (POPG) bilayers, while four amphipathic model peptides remain exclusively on the outer monolayer. The topology of the amphipathic peptide melittin bound to POPC could not be determined because it induced rapid flip-flop of lysoMC. Interestingly, melittin did not induce lysoMC flip-flop in POPG vesicles and was found to remain stably on the external monolayer.

Peptide model systems are increasingly being used for the elucidation of the principles of the insertion, folding, and structure of proteins and peptides in membranes (reviewed in *1*−*4*). A critical issue is the topology of peptides incorporated into lipid bilayers: does a particular model peptide equilibrate freely across the bilayer, form a stable transmembrane structure, or remain only on one surface? The answer to this question clarifies the physicochemical state of a peptide in membranes and thus bears upon the biological activity of peptide model systems. The question is infrequently addressed, however, because there are only a few reliable methods for answering it. The methods fall into three classes. The most widely utilized methods include oriented diffraction (*5*), NMR (*6*), and infrared (*7*, *8*) or circular dichroism (*9*) spectroscopy. For equilibrium systems, these methods can readily distinguish transmembrane orientations from surface orientations, but require that the peptides be incorporated into bilayers oriented on surfaces. The second class of methods is based on measurements of the ability of peptides on one side of a membrane to gain access to the aqueous phase on the opposite side, which implies translocation across the membrane. Examples include assays of translocation by dialysis (*10*) and enzyme digestion (*11*, *12*). The third class is based on the use of lipid-linked probes distributed asymmetrically across lipid vesicles that are capable of quenching the fluorescence of tryptophan residues through resonance energy transfer (RET)[1] (*13*, *12*). Provided the probes remain asymmetric, they can give information about topology through the distance-dependent Förster mechanism of fluorescence quenching by the probe (*14*, *15*). We present here a novel implementation of this third class

[†] Research supported in part by the National Institute of General Medical Sciences (GM-46823).

[‡] Current address: Department of Biochemistry SL-43, Tulane University Medical School. New Orleans, LA 70112.

* To whom correspondence should be addressed. Telephone: 949-824-7122. Fax: 949-824-8540. E-mail: SHWhite@uci.edu.

[1] Abbreviations RET, resonance energy transfer; FRET, fluorescence resonance energy transfer; POPC, 1-Palmitoyl-2-oleoyl-*sn*-glycero-3-phosphocholine; POPG, 1-palmitoyl-2-oleoyl-*sn*-glycero-3-phosphoglycerol; lysoPE, 1-palmitoyl-2-hydroxyl-*sn*-glycero-3-phosphoethanolamine; methylcoumarin, 7-hydroxyl-4-methylcoumarin-3-acetic acid; lysoMC, N-(7-hydroxyl-4-methylcoumarin-3-acetyl)-1-palmitoyl-2-hydroxy-*sn*-glycero-3-phosphoethanolamine; TOE, tryptophan octyl-ester; TOA, tryptophan-octyl-amide; NBD-PE, N-(7-nitrobenz-2-oxa-1,3-diazol-4-yl)-1-palmitoyl-2-oleoyl-sn-glycero-3-phospho-ethanolamine; c.m.c., critical micelle concentration; Ac-18A-NH_2, Ac-DWLKAFY-DKVAEKLKEAF-NH_2; Ac-18A1-NH_2, Ac-ELLEKWAEKLAALK-EALK-NH_2; Ac-18A2-NH_2, Ac-ELLEKWKEALAALAEKLK-NH_2; Ac-18AY-NH_2, Ac-ELLKAWKEALEALKEKLA-NH_2; melittin, GI-GAVLKVLTTGLPALISWIKRKRQQ-NH_2; LUV, large unilamellar vesicles.

10.1021/bi991836l CCC: $19.00
Published on Web 00/00/0000 PAGE EST: 9.8

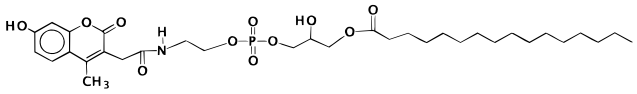

FIGURE 1: Chemical structure of *N*-(7-hydroxyl-4-methylcoumarin-3-acetyl)-1-palmitoyl-2-hydroxy-*sn*-glycero-3-phosphoethanolamine (lysoMC) used for the determination of topology by means of resonance energy transfer (RET). See Materials and Methods for details of synthesis. The lyso-PE moiety anchors the fluorescence-quenching methylcoumarin moiety to the bilayer interfacial region.

of methods, commonly, but inaccurately, referred to as fluorescence resonance energy transfer (FRET). Our implementation of the method overcomes several difficulties, such as the insolubility of probes linked to diacyl lipids and the lack of controls for the loss of probe asymmetry in the course of an experiment. We show how the topology of tryptophan residues confined to the bilayer interfaces of lipid vesicles can be determined by fluorescence quenching using a quencher that is also confined to the bilayer interface. We designed and synthesized a quencher for this purpose, N-(7-hydroxyl-4-methylcoumarin-3-acetyl)-1-palmitoyl-2-hydroxy-*sn*-glycero-3-phosphoethanolamine, that consists of a methylcoumarin fluorophore, an acceptor for Trp fluorescence, linked to the headgroup of lyso-phosphatidylethanolamine (lysoMC, Figure 1). By using a lyso-phospholipid as the membrane anchor for the quencher, we circumvented most of the potential problems of asymmetric lipid quenchers, such as incomplete or nonequilibrium incorporation of the probe into the vesicle membrane. Furthermore, because lysoMC was found to be readily exchangeable between vesicles, it was possible to examine the critical issue of the stability of the transbilayer asymmetry of the probe.

Three physical principles underlie the assessment of the topology of Trp-containing peptides by the lysoMC-RET method described here. First, there is an abundance of physical evidence that tryptophan analogues, as well as Trp residues in proteins and peptides, preferentially interact with membrane interfaces rather than the hydrocarbon core (*16*−*18*). A consequence of this is that membrane-bound tryptophans in the inner and outer monolayers of bilayers are likely to be in equivalent interfacial locations, but separated by the hydrocarbon core thickness of ∼30 Å (*19*). This assumption, readily testable by fluorescence spectroscopy (*20*, *21*), was found to be correct for the compounds we examined. Second, the sixth-power distance-dependence of RET (*14*) suggested the possibility that the quenching of interfacial tryptophans by interfacial quenchers could be largely confined to the same monolayer with only minor contributions from quenchers in the opposing monolayer, and thus impart a strong sidedness to the quenching that could be utilized for the determination of topology. LysoMC was found to have exactly this property. Third, lyso-phospholipids can strongly adsorb to vesicles, while having at the same time the ability to exchange readily between vesicles. Furthermore, because they also form micellar dispersions in water (*22*), solubility problems associated with diacyl phospholipids can be circumvented. Finally, their transbilayer exchange rate (flip-flop) in diacyl phospholipid vesicles is low [$t_{1/2}$ ∼ days (*23*, *24*)]. We thus expected, and in fact found, that we would be able to incorporate lysoMC stably into lipid vesicles either symmetrically (both bilayer leaflets) or asymmetrically (outer bilayer leaflet). For symmetric labeling, lysoMC was mixed with the phospholipids prior

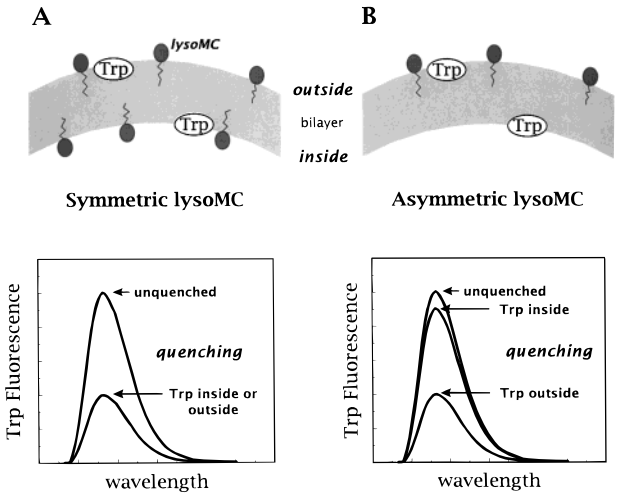

FIGURE 2: Schematic representation of the lysoMC−RET method for the determination of the topology of membrane-bound tryptophan by RET. LysoMC can be easily incorporated into large unilamellar vesicles either symmetrically into both bilayer leaflets at the time of vesicle formation (panel A), or asymmetrically into the outer leaflet by addition to the aqueous phase after vesicle formation (panel B). Comparisons of the fluorescence efficiency *E* of tryptophan in these two types of vesicles (eq 1), quantitated by the *T*-value (eq 6), reveal the topology of the tryptophan as shown in the bottom panels: If the quenching is the same in the symmetric and asymmetric vesicles ($T \sim 1$), then the Trp must be on the outer leaflets of the vesicles where the local lysoMC concentration is the same. If the quenching in the asymmetric vesicles is less than in the symmetric vesicles ($T \sim 0.5$), then some of the Trp must be on the inner leaflet where the local concentration of lysoMC is zero. Intermediate values of *T* will arise when the Trp is present to some extent in both monolayers or is located at the center of the bilayer.

to vesicle formation. For asymmetric labeling, it was added as a micellar suspension after vesicle formation (lysoMC rapidly absorbs to the outer vesicle surface, which reduces the aqueous lysoMC concentration to below the c.m.c.).

Figure 2 shows schematically how we took advantage these three properties for the unequivocal determination of Trp topology using symmetrically and asymmetrically distributed lysoMC (panels A and B, respectively). Schematic fluorescence spectra show the quenching of Trp donors by lysoMC acceptors. In panel A, the symmetrically distributed lysoMC quenches Trp in either bilayer leaflet equivalently, causing the two quenched Trp spectra to be identical. For lysoMC asymmetrically distributed in the outer leaflet, on the other hand, the quenched Trp spectra depend on the sidedness of the Trp (panel B). There is only modest quenching when Trp is on the inner leaflet, but very strong quenching when on the outer leaflet. The sidedness of Trp in vesicles with asymmetric lysoMC thus defines the degree to which a particular Trp is quenched by lysoMC. The method uses Trp-quenching by symmetrically distributed lysoMC as a control and calibration, thus making it unnecessary to know the precise value of the Förster RET distance R_0. One might expect in some cases for Trp to be distributed with less-than-perfect asymmetry. In that case, the quenching should be intermediate between the two extremes shown in panel B.

In this report, we first demonstrate the spectroscopic properties that make lysoMC a good quencher of membrane-bound tryptophan using several examples of the quenching

of membrane-bound Trp by lysoMC. We then describe a critical control experiment for determining the tendency of asymmetric lysoMC to equilibrate across membranes in the presence of peptides. Finally, we show several examples of the determination of topology using lysoMC quenching, including tryptophan analogues and Trp-containing amphipathic peptides.

MATERIALS AND METHODS

Materials. POPC, POPG, and lysoPE were purchased from Avanti Polar Lipids (Alabaster, AL). Melittin and TOE were purchased from Sigma (St. Louis, MO). 7-Hydroxyl-4-methylcoumarin-3-acetyl-succinamidyl ester was purchased from Molecular Probes (Eugene, OR). The peptides Ac-18A-NH_2, Ac-18A1-NH_2, Ac-18A2-NH_2, and Ac-18AY-NH_2 were a gift from V. Mishra and J. Segrest (University of Alabama at Birmingham, AL). The buffer (pH 7.0) used in all experiments was 10 mM HEPES, 50 mM KCl, 1 mM EDTA, and 3 mM NaN_3.

Synthesis and Purification of Tryptophan Octylamide (TOA). TOA was synthesized by coupling 50 mg of *N*-acetyl-L-tryptophan to a 4-fold molar excess of *n*-octylamine in the presence of a 4-fold excess of *N*-methylmorpholine, hydroxybenzotriazol, and benzotriazole-1-yl-oxy-tris-pyrrolidino-phosphonium-hexafluorophosphate. TOA was purified to >99% by reverse-phase HPLC using a C8 column. The product was stored at −20 °C as a methanol stock solution.

Synthesis and Purification of LysoMC. LysoMC was synthesized by covalently attaching the methylcoumarin probe to the primary amino group of the lysoPE headgroup. This was accomplished by reacting 20 mg of 7-hydroxyl-4-methylcoumarin-3-acetyl-succinamidyl ester with 20 mg of 1-palmitoyl-2-hydroxy-*sn*-glycero-3-phosphoethanolamine (lysoPE) in 2 mL of methanol at pH 8 for 1 h. About 50% of the lysoPE was converted to lysoMC by attack of the reactive coumarin-succinnamidyl ester on the ethanolamine nitrogen. The lyso-phospholipids were separated from all the other reactants and products by means of C8 reverse-phase HPLC using water−acetonitrile gradients. LysoMC was separated from lysoPE using preparative thin-layer chromatography in a solvent system consisting of 65% $CHCl_3$, 30% CH_3OH, 2.5% H_2O, 2.5% NH_4OH. LysoPE remained near the origin ($R_f \sim 0.1$) and lysoMC migrated with a $R_f \sim 0.7$. Purified lysoMC was stored in $CHCl_3$ at −20 °C and was found by analytical thin-layer chromatography and fluorescence to be chemically stable for more than 12 months.

Fluorescence. Fluorescence was measured using a SLM/Aminco 8100 steady-state fluorescence spectrometer (Spectronic Instruments, Rochester, NY). All measurements were made in 4 × 10 mm cuvettes at an ambient temperature of 22 °C. In all cases, polarizers were used in a magic angle configuration (excitation polarization set to 54.7° relative to vertical, emission polarization set to vertical) in order to correct for polarization effects in measurements of intensity, reduce direct contributions of light scattering, and eliminate polarization effects in monochromator transmittance. Tryptophan fluorescence was excited at 260 nm with slits set to 4 nm. Direct fluorescence of lysoMC was excited at 330 nm and measured at 450 nm. We prevented photobleaching of lysoMC by using 1 nm excitation slits. Emission spectra were not corrected for instrumental response, because we have found that such corrections have negligible effects on the shape of Trp fluorescence spectra, based upon comparisons with the standard Trp spectrum of E. A. Burstein [see Permyakov, ref *25*].

Resonance Energy Transfer Quenching. Quenching experiments are usually quantitated using standard formulas (*15*). Briefly, the experimental transfer efficiency (E) of quenching is described by

$$E = 1 - (F_q/F_0) \quad (1)$$

where F_0 is the unquenched fluorescence intensity and F_q the intensity in the presence of the quencher. The relation of E to the distance r between donor (tryptophan) and acceptor (lysoMC) is based upon the equation

$$E_{pair} = R_0^6/(R_0^6 + r^6) \quad (2)$$

where R_0 is the Förster distance and E_{pair} is the efficiency for donor−acceptor pairs separated by a fixed distance (*15*). To be able to distinguish between Trp residues on the inner and outer surfaces of a bilayer vesicle, the effective R_0 should be about equal to the thickness d_{HC} of the bilayer's hydrocarbon core. In the method outlined here, however, the precise value of R_0 does not matter. Nevertheless, it is important to establish that the effective R_0 is in fact comparable to d_{HC}.

The Förster distance for donors and acceptors in solution is generally computed from (*15*)

$$R_0 = 9.79 \times 10^3(\kappa^2 n^{-4} \phi_d J)^{1/6} \text{ Å} \quad (3)$$

where κ^2 describes the relative orientations of acceptor and donor, n is the refractive index of the medium, ϕ_d the quantum yield of the donor, and J the overlap integral that describes the spectral overlap between the donor emission and the acceptor absorption. If the donor and acceptor are isotropically oriented, as frequently assumed, then $\kappa^2 = 2/3$.

Equations 1−3 are most frequently applied to donors and acceptors separated by a fixed distance. This is a reasonable assumption for labeled proteins, for example, but it is does not take into account membrane systems that have donors and acceptors randomly distributed on the quasi-2-dimensional membrane surface. The constraints imposed by the surface might also cause the donors and acceptors to lie at different depths in the membrane (which affects the computation of r) or not to be isotropically oriented ($\kappa^2 \neq 2/3$). RET quenching in membrane systems has been considered in detail by Wolber and Hudson (*26*) and Davenport et al. (*27*). The effect on R_0 of various assumptions about κ^2 in membrane systems with Trp donors was examined in detail by Ladokhin et al. (*28*) who found that R_0 was affected only moderately by the choice of κ^2 in a study of Trp quenching in cytochrome b_5. For example, they found that values of κ^2 were limited to a range of 0.28−1.75, resulting in R_0 values of 25−34 Å. The extreme thermal motion inherent to fluid bilayers (*19*) and the resulting high mobility of the acceptors and donors used our studies suggests that isotropic averaging is an appropriate assumption. In any case, our lysoMC−RET method requires only that $R_0 \sim d_{HC}$, so that $\kappa^2 = 2/3$ is a reasonable choice. Wolber and Hudson (*26*) made the same choice in their analysis.

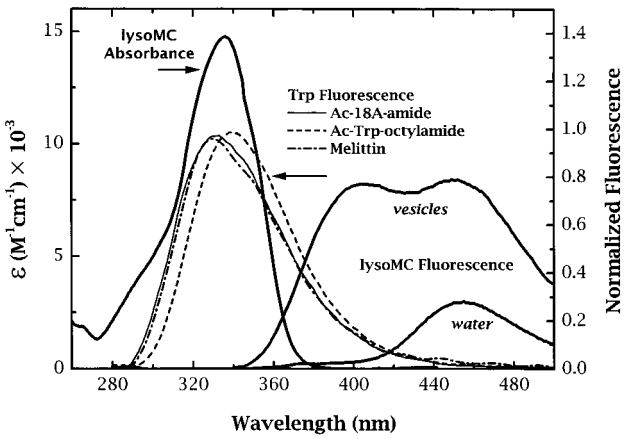

FIGURE 3: Spectroscopy associated with RET between tryptophan and lysoMC. The absorbance spectra of lysoMC is characterized by a maximum at 335 nm with $\epsilon = 14\,900\ M^{-1}\ cm^{-1}$ (curve on far right). The normalized fluorescence emission spectra (260 nm excitation) of *N*-acetyl tryptophan octylamide (TOA) and of the amphipathic peptides Ac-18A-NH_2 and melittin in membranes are shown in the center set of curves. The good overlap between the lysoMC absorbance and membrane Trp emission gives rise to an R_0 value of ~25 Å which demonstrates that lysoMC is a good short-range RET quencher of Trp fluorescence in membranes (see text). The curves on the far right show the direct fluorescence emission of lysoMC (excited directly at 330 nm) when partitioned into vesicles (1 mol %) and into water where it is micellar. The shapes of the two curves differ, probably because of methylcoumarin self-quenching in the micellar form (see text). The exact shape of the lysoMC fluorescence curves is unimportant in our experiments because topology is assessed from the Trp fluorescence (see text).

To establish that eqs 2 and 3 approximately described RET between Trp and lysoMC in our LUV system, we used the analysis of Wolber and Hudson (*26*) to test the hypothesis that eq 2 adequately described the experimentally observed quenching of eq 1. In addition, we devised an easily implemented numerical simulation of the Wolber−Hudson approach that may be generally useful. As shown in Results, our simulation gave results similar to the Wolber−Hudson analysis. Both approaches showed that *E* of eq 1 was well described by E_{pair} of eq 2 in our experiments.

The values of R_0 computed according eq 3 were found to be about the same for TOA, TOE, and the tryptophans of the peptides: ≈25 Å. In our system, using the quantum yield of Trp in water of 0.14 (*29*) as the reference (*30*), we found that ϕ_d ranged between 0.1 and 0.2. *J* was computed from data such as those of Figure 3, κ^2 was taken as $^2/_3$, and *n* as the index of refraction of water. Possible sources of error in the calculation of R_0 include uncertainties in κ^2 (see above), choice of *n*, and the estimate of ϕ_d (due to differences in spectral shape and position of our compounds compared to the tryptophan standard). We estimated that, together, these uncertainties might cause R_0 to be uncertain by ~5 Å. We thus expected the true R_0 for the Trp-lysoMC donor−acceptor system to lie between 20 and 30 Å. Any value within this range was acceptable because we only require that $R_0 \sim d_{HC}$.

A Simple Numerical Simulation of RET for Membrane-Bound Donors and Acceptors. A Pascal program was written to implement the following algorithm (the program is freely available from the authors). A 500 × 500 "square" lattice (2.5×10^5 sites) with spacing *h* was used to calculate distances in terms of the number of lattice sites multiplied by a constant lattice parameter $h^2\pi$. We used $h = 4.72$ Å, equivalent to the lipid−lipid spacing of fluid-phase membranes (*31*). This yielded a lattice parameter of 70 $Å^2$. The number of desired acceptors *N* in a particular simulation run was computed from the target mol-fraction of acceptor (*f*) using $N = 2.5 \times 10^5 f$. For a given choice of *f*, N_j acceptors were scattered randomly on the lattice. We made the simplifying assumption that there was no lateral diffusion on the time scale of the Trp excited state. Possible differences in depth of donor and acceptor were also ignored in the final version of the simulation because the effect of including them was negligible for the acceptor concentrations used in our experiments. Wolber and Hudson (*26*) derived a mathematical expression for the relative quantum yield of a donor surrounded a particular configuration of receptors. Adapting their expression (cf. eq 4) leads to

$$F_j = [1 + \sum_{i=1}^{N_j}(R_0/r_i)^6]^{-1} \quad (4)$$

where F_j is the fluorescence arising from a donor fluorophore separated from the i^{th} acceptor by a distance r_i.

Note that for high acceptor dilution for which all r_i become large compared to R_0, $F_j \rightarrow 1$. For each value of *f*, $M = 100$ trials were performed ($j = 1...M$). The average fluorescence $\bar{F}(f)$ was computed as a simple average from

$$\bar{F}(f) = \frac{1}{M}\sum_{j=1}^{M} F_j \quad (5)$$

RET Measure of Topology. The lysoMC−RET method relies upon a comparison of the quenching efficiency E_{asym} observed in asymmetrically labeled vesicles with the efficiency E_{sym} observed in symmetrically labeled vesicles (Figure 2). Such a comparison makes the method largely independent of the precise value of R_0. For this purpose, we define the *T*-value

$$T = E_{asym}/E_{sym} \quad (6)$$

The interpretation of a value *T* follows from a consideration of Figure 2. A value of $T \sim 1$ is unequivocal: the tryptophan has remained on the outer monolayer of the vesicles. Values of *T* smaller than 1 can only result from the redistribution of Trp across the membrane so that it is present in both monolayers. An equilibrium distribution will give rise to $T \sim 0.5$.

Vesicle Preparation. Large unilamellar vesicles of diameter 0.1 μm were prepared by extrusion (*32*, *33*) from either POPC or POPG. Vesicles with symmetrically distributed lysoMC were made by adding 1 mol % lysoMC to the phospholipids in organic solvent, followed by vacuum-drying, hydration, and vesicle preparation. Asymmetric vesicles were made by adding 0.5 mol % (total) lysoMC, dispersed in buffer, to a solution of preformed vesicles. The lysoMC partitions into the outer monolayer of the vesicles, giving a local concentration of 1 mol % lysoMC. The concentration of lysoMC in the two types of vesicles was assayed by measuring lysoMC fluorescence. The absolute concentrations were always equal to the expected value, and the ratio of concentration in the asymmetric vesicles to the symmetric vesicles was always between 0.47 and 0.53.

Intervesicular Exchange of LysoMC. Intervesicular exchange of lysoMC was measured to ascertain the transbilayer diffusion (flip-flop) rate of lysoMC. Two types of vesicles were used in this assay: donor vesicles containing initially 1 mol % lysoMC and acceptor vesicles containing 1 mol % NBD-PE, which is a nonexchangeable quencher of lysoMC fluorescence. In an exchange experiment, the lysoMC fluorescence in a 25 μM solution of lysoMC-containing donor vesicles was determined and then monitored after the addition of a 10-fold excess of NBD-PE-containing acceptor vesicles. The lysoMC that was exposed to the outer monolayer of the donors exchanged rapidly into the acceptors, where its fluorescence was quenched (see Results). The extent of lysoMC exchange was ascertained by comparing the final level of lysoMC fluorescence with that expected for complete exchange. The lysoMC fluorescence for complete exchange was ~0.42, as determined by experiments with asymmetric (i.e., completely exchangeable) lysoMC or in experiments with alamethicin-induced flip-flop. In exchange experiments with peptides or Trp-analogues, these compounds were added to the donor vesicles prior to the exchange experiment.

Determination of Tryptophan Topology. Determination of Trp topology was performed by measuring Trp fluorescence in vesicles containing 1 mol % of symmetrically distributed lysoMC and comparing it with the fluorescence of vesicles containing either no lysoMC or 1 mol % in the outer monolayer only (0.5 mol % total). The analysis is shown schematically in Figure 2 and discussed in detail below. The experiment was performed as follows. The Trp-containing compound was added to buffer at a concentration of 1−15 μM in each of two cuvettes. Into one cuvette an aliquot of pure lipid vesicles was added and into the other the same amount of vesicles containing 1% symmetric lysoMC. After equilibration for ~15 min, the fluorescence spectra were recorded. Next, an aliquot of lysoMC, dispersed in buffer, was added to the pure lipid sample to bring the total concentration to 0.5 mol % (1 mol % in the outer monolayer). After 1−15 min of equilibration, the fluorescence spectrum of this sample was measured and compared to the others as described in the text (see Figure 2). In all cases, we established beforehand that more than 80% of the Trp-containing compounds was bound to the vesicles under these experimental conditions and that the asymmetric lysoMC remained stably asymmetric for the duration of the measurements.

RESULTS

RET Spectroscopy. The choice of 7-hydroxyl-4-methylcoumarin-3-acetic acid as the RET acceptor in these experiments was based on its expected ability to quench the fluorescence of membrane-bound tryptophan. As shown in Figure 3, the absorbance maximum of lysoMC ($\epsilon = 14\,950$ M^{-1} cm^{-1}) at 335 nm gives good spectral overlap with the fluorescence emission of the Trp of several membrane-bound compounds (Ac-18A-NH_2, melittin, and TOA). This results in efficient resonance energy transfer characterized by the Förster distance R_0 (*15*), which we found to be ~25 Å for all Trp-containing compounds examined (see Methods).

The fluorescence emission spectra of lysoMC in water and vesicle membranes, directly excited at 330 nm, are also shown in Figure 3. Interestingly, the spectrum is bimodal in vesicles, despite the predominantly unimodal absorbance peak. Methylcoumarin alone in water also has a bimodal fluorescence emission spectrum (data not shown), probably due to an excited-state reaction. Interestingly, the fluorescence spectrum of lysoMC in water is unimodal. The unimodal spectrum probably arises from some form of self-quenching due to the micellar state of lysoMC in water in the absence of vesicles, but the exact origin is not known. The unimodal character was observed at concentrations down to 5 nM, suggesting that the c.m.c. is less than this value. Whatever the origin of the bimodal spectrum of lysoMC emission, its exact shape does not affect the results presented here.

The lysoMC absorbance spectrum shown in Figure 3 indicates significant absorbance below 280 nm, in the same region as direct excitation of Trp. This means that in addition to RET excitation of lysoMC in our experiments, lysoMC was also being excited directly. An examination of the intensities of Trp and lysoMC fluorescence as a function of excitation wavelength revealed that the ratio F_{Trp}/F_{lysoMC} was maximum at 260 nm, which explains the choice of 260 nm as the excitation wavelength in our experiments. The direct excitation of lysoMC would complicate the RET measurement if one were to use only the changes in lysoMC fluorescence as a measure of topology. However, one can also quantitate RET by measuring the quenching of Trp fluorescence. This is preferable because a close examination of Figure 3 reveals that the low wavelength edge of the emission bands of lysoMC does not extend to below ~340 nm under any conditions. This property, and the very short range of effective RET explains why the addition of lysoMC has no effect on the low wavelength (λ < 340 nm) fluorescence of tryptophans that are not membrane bound (data not shown). Consequently, we quantitated RET using quenching efficiency E (see Methods) with Trp fluorescence intensities measured at a constant wavelength (either the emission maximum or at 335 nm, whichever was lower).

Partitioning of lysoMC into Membranes. Lyso-phospholipids with palmitate chains were expected to form micelles in aqueous solution in the absence of bilayers and to become rapidly incorporated into added vesicle membranes (*31*, *34*). We found that lysoMC indeed has these properties. For instance, lysoMC in aqueous buffer formed clear nonviscous solutions at all concentrations between 5 nM and 5 mM, consistent with the formation of micelles. The apparent self-quenching of lysoMC fluorescence in water keeps its fluorescence intensity low compared to its intensity when partitioned into vesicles. The addition of 10 μM vesicles to 5 nM lysoMC caused a large, rapid (<1 min) increase in fluorescence, due to the relief of self-quenching that occurred when the lysoMC became incorporated into the vesicles. Further additions of lipid had negligible effects on the lysoMC fluorescence, indicating that binding was essentially complete at lipid concentrations much lower than the ones used in the topology and exchange experiments (typically 0.5−1 mM, see below). In a converse experiment, we added lysoMC dispersed in buffer to a solution of vesicles and found no self-quenching because of the rapid and apparently complete incorporation of lysoMC into the vesicle bilayers. The fluorescence increased linearly with further additions of lysoMC up to about 2 mol %. Intervesicular exchange

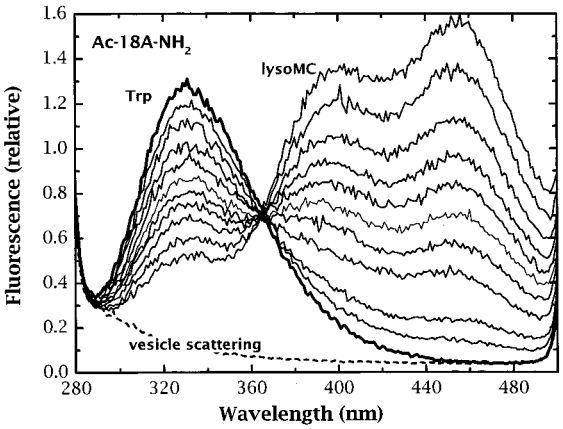

FIGURE 4: Fluorescence of Ac-18A-NH_2 (5 μM) in POPC vesicles (1 mM) titrated with lysoMC. Fluorescence was excited at 260 nm. The fluorescence emission peak at 330 nm is from the Trp of Ac-18A-NH_2. The two fluorescence emission peaks at 400 and 450 nm are from lysoMC. Trp fluorescence in the absence of lysoMC is shown as a thick line. LysoMC, added from a aqueous stock solution, causes a smooth decrease in Trp fluorescence with a distinct isoemissive point at 360 nm, suggesting a lack of complex or coöperative interactions. The lower dashed curve is the background scattering signal from POPC vesicles alone. Both lysoMC and Ac-18A-NH_2 stay on the outer bilayer leaflets of the vesicles during these measurements (see text). The mole fractions of lysoMC corresponding to each curve, progressing from bottom to top, are given by the points plotted in Figure 5.

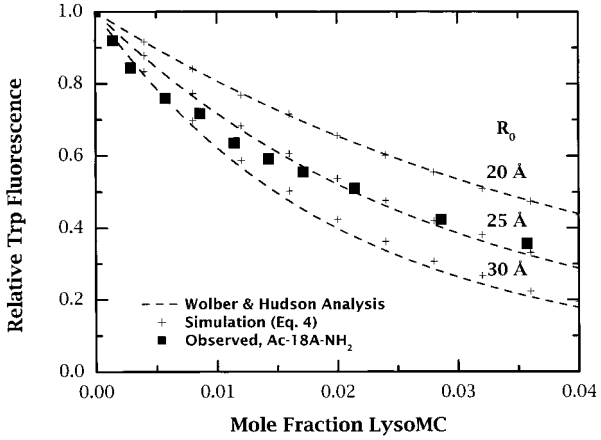

FIGURE 5: The concentration-dependence of the quenching of Ac-18A-NH_2 by lysoMC. These data were taken from the titration experiment shown in Figure 4. The relative fluorescence shown here is the background-corrected intensity at the emission maximum divided by the corrected intensity in the absence of lysoMC. The mole fraction of lysoMC is the concentration on the outer monolayer. For comparison, quenching curves computed according to the to the analysis of Wolber and Hudson (*26*) are shown as dotted lines for $R_0 = 20$, 25, and 30 Å. The results of simulations using the simple algorithm described in Methods (eqs 4 and 5) are shown by the plus signs (+). The agreement of the two analyses is quite good. We calculated from the spectroscopic properties that $R_0 \sim 25$ Å (Figure 3). Given the uncertainties in the calculations of R_0 in membrane systems (*15*), the agreement between the theoretical and measured quenching is excellent.

experiments (see below) demonstrated that lysoMC also rapidly exchanged between vesicles. We concluded that the aqueous concentration of lysoMC was negligible under the conditions of our experiments.

Tryptophan Quenching by lysoMC. The quenching of Trp by lysoMC is illustrated in Figure 4, which shows the result of titrating a mixture of POPC vesicles + Ac-18A-NH_2 with lysoMC. The titration resulted in a large and progressive decrease in tryptophan fluorescence and a concomitant increase in lysoMC fluorescence. The isoemissive point at 360 nm, observed in all of our quenching experiments for all of the Trp-containing compounds, is somewhat surprising because the lysoMC fluorescence results from both direct excitation and RET (see above) and one does not expect the RET efficiency to increase linearly with lysoMC concentration. As discussed below, the apparent Förster distance R_0 appears to depend somewhat upon lysoMC concentration. This, some other nonlinearity, and the very strong contribution (>50%) of direct excitation to lysoMC fluorescence may conspire to cause an apparent isoemissive point. The concentration dependence of lysoMC quenching, shown by the closed squares (■) in Figure 5, was very similar to that for the other Trp-containing compounds, as summarized in Table 1. The concentration of lysoMC in the symmetric vesicles was 1 mol % in all cases. The efficiencies of quenching for the compounds shown in Table 1 range from 0.33 to 0.49.

Three simulated quenching curves were computed from an analytical expression derived for dilute solutions by Wolber and Hudson (*26*) (cf eq 17) and by the numerical procedure described in Methods using $R_0 = 20$, 25, and 30 Å. The Wolber−Hudson analytical expression yielded the dashed curves shown in Figure 5. The results of our numerical simulations are shown by the plus signs (+) in the figure. The agreement between the two approaches is excellent and both are in reasonable agreement with the experimental data. The deviation of the data from the simulated curves suggests an apparent concentration dependence of the Förster distance, R_0 being larger at low concentrations. This may reflect, however, inadequacies of the models. Overall, we concluded that $R_0 \sim 25$ Å was a reasonable value and that eq 3 provided a good estimate of R_0 even for RET on membrane surfaces, at least under our experimental conditions. We do not know if this agreement will hold true for other donor−acceptor systems.

Transbilayer Exchange and Distribution of lysoMC. To determine the topology of a membrane-bound tryptophan by RET, one must establish that asymmetrically distributed lysoMC in vesicles remains asymmetric for at least the few minutes required to make the fluorescence measurements. This is an especially important consideration for vesicles containing membrane-active peptides such as melittin because several peptides of this type have been shown to induce flip-flop of lipid-linked probes (*35*, *36*). We used a simple lipid exchange procedure to examine the flip-flop of lysoMC under different conditions. In brief, lysoMC-free acceptor vesicles containing the nonexchangeable quencher NDB-PE were injected into the cuvette with the lysoMC-labeled donor vesicles (see Methods). The rate of flip-flop was assessed by measuring the fraction of lysoMC that was exchangeable (i.e., taken up by the acceptor vesicles) (*37*, *38*) as judged by the reduction in the lysoMC fluorescence. If flip-flop was rapid, then essentially 100% of the lysoMC would be exchangeable, whereas if flip-flop was slow, then only the 50% on the outer monolayer would be exchangeable, while the 50% on the inner monolayer would be nonexchangeable.

Figure 6 shows the results of exchange experiments for lysoMC symmetrically incorporated into POPC LUV (solid curves). The exchange with acceptor vesicles was rapid, but

Table 1: Summary of the Determination of the Topology of Various Tryptophan-containing Compounds Using the LysoMC−RET Method

	POPC				POPG			
compound	λ_{max}[a]	E[b]	T[c]	flip-flop[d]	λ_{max}[a]	E[b]	T[c]	flip-flop[d]
TOA[e]	339	0.45	0.61	no	333	0.37	0.56	no
TOE[f]	335	0.48	0.61	no	332[f]	0.33	0.59	no
Ac-18A-NH_2[g]	328	0.37	1.03	no	323	0.35	1.10	no
Ac-18A1-NH_2[g]	n.o.[h]	n.o.[h]	n.o.[h]	no	325	0.38	1.00	no
Ac-18A2-NH_2[g]	n.o.[h]	n.o.[h]	n.o.[h]	no	321	0.49	1.08	no
Ac-18AY-NH_2[g]	n.o.[h]	n.o.[h]	n.o.[h]	no	324	0.43	1.06	no
melittin	327	0.45	n.a.	yes	327	0.43	1.03	no
alamethicin[i]	n.o[i]	n.o[i]	n.o[i]	yes	n.o[i]	n.o[i]	n.o[i]	yes

[a] Wavelength of fluorescence emission maximum (nm). [b] Efficiency (E) of quenching of tryptophan fluorescence in vesicles containing 1 mol % of symmetric lysoMC (see text). [c] Ratio of E of symmetric and asymmetric quenching, $T = E_{asym}/E_{sym}$. Experimental uncertainties in T depend on the peptide concentrations but range from 3% to 6%. [d] Transbilayer exchange of lysoMC caused by the Trp-containing compounds present at about 0.5−2 mol % in the membrane. [e] Acetyl tryptophan octyl amide. [f] Tryptophan octyl ester. The emission maximum of TOE depends on membrane concentration in POPG vesicles, ranging from 325 to 342 nm. The value of 332 nm is thus a nominal value that depends on concentration. However, the value of the emission maximum had no effect the T-value. [g] 18 residue amphipathic helix (*48*, *49*). [h] Not observable because these peptides do not bind strongly enough to POPC LUV. [i] Not observable because alamethicin does not have tryptophan, but was assayed for its ability to cause transbilayer equilibration of lipids.

the extent was only 50% as large as the complete-exchange equilibrium expectation (heavy dot−dash line; see Methods). This is consistent with the expectation that lysoMC on the inner leaflet of the vesicles was not exchangeable on a half-hour time scale. For lysoMC freshly incorporated asymmetrically into the outer monolayer of POPC vesicles (fine-dashed curve), the exchange was likewise rapid, but the extent was 100%. This is the expected result for all of the lysoMC being on the outer monolayer of the vesicles. Incubation of these vesicles for 24 h or more after lysoMC incorporation had no effect on the extent of exchange. We conclude from these experiments that the inherent transbilayer exchange (flip-flop) of lysoMC occurred with half-times significantly longer than 24 h.

To confirm that the nonexchangeable lysoMC of symmetric donor vesicles is in the inner monolayer, we tested various peptides and detergents for an exogenous compound that would induce the exchange of the remaining 50% of the probe, presumably through bilayer perturbations/destabilization. As expected from early work with planar bilayer films (*39*), we found that 0.5 mol % of the pore-forming antibiotic peptide alamethicin, added after the initial exchange, had this effect in POPC (Figure 6) and POPG (data not shown). If the alamethicin was added before the addition of acceptor vesicles, then the initial extent of exchange was 100% instead of 50%. In all cases, a second addition of alamethicin had no effect. These results provide further support for our conclusion that lysoMC incorporated asymmetrically into peptide-free POPC or POPG membranes remained stably asymmetric for days.

Because alamethicin caused lysoMC flip-flop, the possibility arose that our Trp-containing compounds would also cause flip-flop. We examined this issue by repeating the alamethicin-type experiment on POPC and POPG LUV using several compounds, including TOA, Ac-18A-NH_2 and related peptides, and melittin (Table 1). With the exception of melittin in POPC vesicles, we found no evidence for the induction of transbilayer exchange of lysoMC. The exchange curve obtained for POPC vesicles with 0.5 mol % melittin is shown in Figure 6. The initial extent of lysoMC exchange was nearly 100%, clearly showing that melittin induced transbilayer exchange of lysoMC. The topology of melittin in POPC can thus not be assayed using lysoMC, or any other variation on the RET experiment that utilizes a lipid associated fluorophore.

Examples of the Determination of Tryptophan Topology. As summarized in Figure 2 and described in detail in Methods, the topology of tryptophan in membranes was determined by comparing Trp fluorescence in pure lipid vesicles to vesicles containing 1 mol % of symmetrically distributed lysoMC or 1 mol % of asymmetrically distributed lysoMC (outer bilayer leaflet) by means of the T-value. The efficiency of quenching of various Trp-containing compounds by symmetric lysoMC ranged from 0.33 to 0.49 (Table 1). Examples of fluorescence-quenching topology experiments are shown in Figures 7, 8, and 9 for, respectively, melittin in POPG, TOA in POPC, and Ac-18A-NH_2 in POPC. Values of E and T for the various compounds examined are presented in Table 1.

The T-values fall into 2 classes: the two hydrophobic tryptophan analogues, TOE and TOA, have $T = 0.5-0.6$, strongly suggesting that they equilibrated across both POPC and POPG membranes. The peptides all had values of $T \sim 1$ in those cases, where binding was sufficiently strong and no flip-flop was induced, indicating a stable external location. In all these cases, the stable equilibrium topology was reached within about 5 min after addition of the vesicles. We expect that if this is not the case for some peptides, that lysoMC method will be well-suited for studying the time dependence of transbilayer movement of tryptophan if the time-scales are in the range of minutes to hours.

DISCUSSION

Our experiments demonstrate that the membrane-bound quencher lysoMC can be incorporated either symmetrically or asymmetrically into phospholipid vesicles and thus used for determining, by means of RET, the topology of Trp-containing compounds partitioned into the vesicles. The method works only if the Trp-containing compounds do not induce lysoMC flip-flop in the manner of alamethicin (POPC and POPG) and melittin (POPC, but not POPG). A simple lipid-exchange procedure using NBD-PE-doped acceptor vesicles allowed this possibility to be tested. The use of lyso-PE as the lipid anchor for the methylcoumarin quencher was exceptionally convenient for these experiments, because it

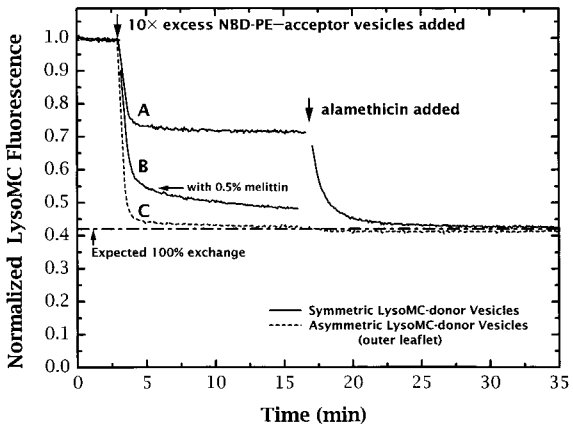

FIGURE 6: Exchange of lysoMC between POPC vesicles in the presence and absence of melittin and/or alamethicin as monitored by the quenching of lysoMC fluorescence by NBD-PE. Three classes of vesicles were used in these experiments: (1) POPC vesicles with 1 mol % symmetric lysoMC, (2) POPC vesicles with 1 mol % asymmetric (outer monolayer) lysoMC, and (3) POPC vesicles labeled with 1 mol % NBD-PE. NBD is a RET quencher (acceptor) of lysoMC fluorescence (donor). Hence, the lysoMC-labeled vesicles and NBD-PE-labeled vesicles are referred to as donor and acceptor vesicles, respectively. NBD-PE does not exchange significantly between vesicles. Exchange of lysoMC from donor to acceptor vesicles is therefore indicated by a decrease in lysoMC fluorescence. The figure shows the results of three experiments (A−C). In all cases, an experiment began at $t = 0$ with lysoMC-labeled donor vesicles in the cuvette (25 μM POPC). A few minutes later, as indicated by an arrow, an excess of NBD-labeled acceptor vesicles was added. After the lysoMC fluorescence had declined to its new value in 10 min or so, alamethicin was added to the cuvette as indicated by a second arrow. A. POPC vesicles alone with symmetric lysoMC. Fluorescence declines halfway toward the 100% exchange level (dot−dash curve), indicating the loss of lysoMC from the outer vesicle surface. The addition of alamethicin induces lysoMC flip-flop which allows completion of exchange, as indicated by the further decline of lysoMC fluorescence to the 100% exchange level. B. The same experiment as in A except that 0.5 mol % melittin was present. The post acceptor-vesicle fluorescence in this case declined to a lower level than in A because melittin caused flip-flop of lysoMC. C. The same experiment as in A except asymmetric lysoMC-labeled vesicles were used. Because the lysoMC was located exclusively in the outer monolayer, it was lost rapidly and completely to the acceptor vesicles, as indicated by the rapid decline of lysoMC fluorescence to the 100% exchange level.

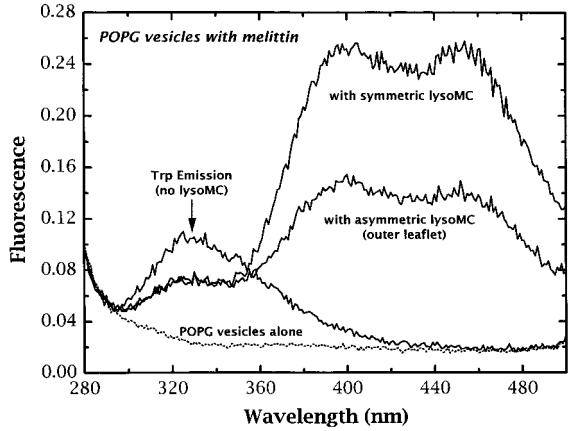

FIGURE 7: Determination of the topology of melittin (0.5 mol %) bound to POPG vesicles (0.5 mM). Four fluorescence spectra were measured in order to determine the topology of melittin's tryptophan in vesicle bilayers: POPG vesicles alone (light-scattering control, dotted line), pure POPG vesicles + melittin, POPG vesicles with asymmetric lysoMC (0.5 mol %) + melittin, and POPG vesicles with symmetric lysoMC (1 mol %) + melittin. The level of Trp fluorescence ($E \sim 0.5$) is the same for both symmetric and asymmetric vesicles so that $T \sim 1$, indicating that melittin is constrained to the outer leaflet of the bilayer. Melittin in POPG does not cause asymmetric lysoMC to equilibrate (flip-flop) across bilayers (Table 1).

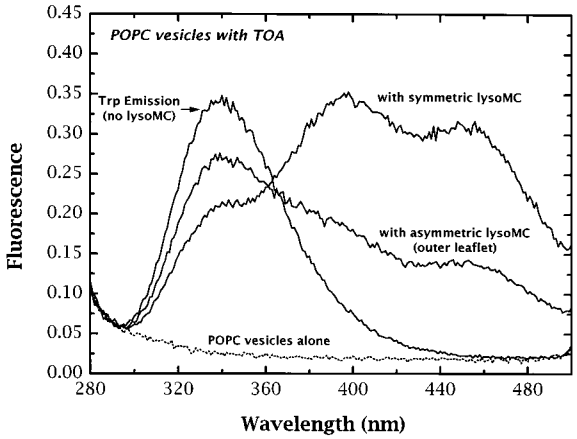

FIGURE 8: Determination of the topology of TOA (2 mol %) in POPC vesicles (0.5 mM). Four fluorescence spectra were measured in the same manner as for melittin, described in the legend of Figure 7. The level of Trp fluorescence is different for symmetric ($E \sim 0.4$) and asymmetric vesicles ($E \sim 0.2$). The fluorescence is higher for asymmetric vesicles because TOA can apparently equilibrate across the bilayer and thereby reduce the quenching effect of lysoMC constrained to the outer bilayer leaflet ($T \sim 0.5$). TOA in POPC does not cause asymmetric lysoMC to equilibrate across bilayers (Table 1).

is "soluble" in water in micellar form but rapidly and completely partitions into lipid vesicles when they are present. This is a distinct advantage over the use of diacyl lipids because lyso-glycerolipids can be incorporated asymmetrically in situ by adding an aliquot of the lipid in buffer to preformed vesicles. Asymmetric incorporation of diacyl lipids is often accomplished by the rapid dilution of an organic solution of lipids into an aqueous solution of preformed vesicles (*12*) with the assumption that rapid mixing will result in homogeneous uptake of the lipid into the vesicles. This is not necessarily a good assumption because rapid precipitation of the quenching lipid can occur. We have observed, for example, that dilution of a methanol solution of diacyl NBD-PE into an excess of POPC vesicles results in a highly self-quenched solution, suggesting that the formation of new vesicles from spontaneous self-association of NBD-PE predominates over the incorporation of NBD-PE into extant vesicles. Redistribution of diacyl lipids among vesicles is also effectively prevented by their slow exchange (*40*, *38*) in contrast to lyso-glycerolipids, which equilibrate rapidly between vesicles (see above).

The obvious case for which the lysoMC−RET method will be misleading is for tryptophans located near the center of the bilayer, where they will be quenched equally by lysoMC on either side of the membrane. This will give rise to an intermediate *T*-value that would suggest, incorrectly, that the tryptophans are equilibrated between the two bilayer leaflets. Fortunately, deeply buried tryptophans can readily be identified because of their distinctive fluorescence spectra that show high quantum yields and emission maxima at wavelengths below 320 nm (*41*, *20*). Most interface-bound

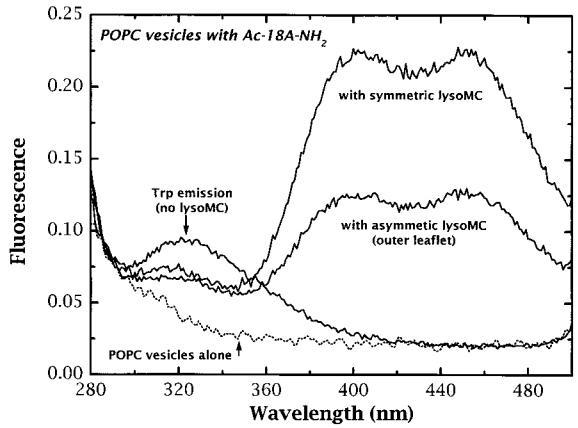

FIGURE 9: Determination of the topology of Ac-18A-NH_2 (0.5 mol %) in POPC vesicles (0.5 mM). Four fluorescence spectra were measured in the same manner as for melittin, described in the legend of Figure 7. The fluorescence spectra are similar to those of the POPG-melittin experiment of Figure 7, indicating that bound Ac-18A-NH_2 resides solely on the outer bilayer leaflet. Ac-18A-NH_2 in POPC does not cause asymmetric lysoMC to equilibrate across bilayers (Table 1).

tryptophans, including all of the compounds in Table 1, have emission maxima at wavelengths between 321 and 339 nm. Another predicted result of a Trp deep in the bilayer interior would be relatively poor quenching by lysoMC, which resides at the bilayer interface. The data in Table 1, however, show that the quenching efficiency of Trp fluorescence by lysoMC ranges narrowly between 0.33 and 0.49, consistent with similar interfacial locations for all of the tryptophans examined (see Figure 3). A Trp in the bilayer center would be as much as 15 Å farther away from the lysoMC plane. Our numerical simulations suggest that in that case E would be $\sim$ 0.05.

Topology of TOA and TOE. By the criteria discussed above, the Trp residues of none of the compounds listed in Table 1 appear to be in the bilayer center so that the T-values accurately reveal their topology. The two tryptophan analogues, TOA and TOE, readily equilibrated across the bilayer, as shown by T-values of 0.55−0.60. Their equilibrium distributions were attained within 1−2 min and were stable for hours. That TOA crosses bilayers so readily is not surprising because most hydrophobic, uncharged molecules do so (*42*). The behavior of TOE, on the other hand, was uncertain prior to these measurements because it carries a charge on its amino group that might be expected to slow transbilayer exchange considerably (*42*). The experimental results shown in Table 1 are unequivocal: TOE equilibrated rapidly and completely across POPC and POPG bilayers. The ability of TOA and TOE to cross the bilayer easily is consistent with the idea that Trp residues of membrane proteins, which have a high propensity for membrane interfaces (*43*, *44*), act as "needles" (*17*) for pulling the transmembrane helices across membranes. Although the Trp side chain has a high inherent physicochemical propensity for the bilayer interface compared to other residues (*43*), probably because of its complex electrostatic properties (*44*), the difference between its whole-residue free energy of transfer from water into bilayer interfaces and into *n*-octanol (*4*) is small. This implies that Trp can readily cross the bilayer, as observed in our experiments.

An interesting sidelight of our experiments was that the T-values for TOA and TOE were slightly larger than 0.50. This is not surprising because TOA and TOE readily cross the bilayer, causing the effective interfacial distribution along the bilayer normal to be quite broad (*45*, *46*). This should increase T due to quenching from the opposing leaflet (trans-leaflet quenching), which should have a larger total effect in asymmetric vesicles that in symmetric ones. Calculations suggest that a trans-leaflet E of 0.1 is sufficient to increase the equilibrium T from 0.50 to 0.56. Second, for vesicles of the size used in these experiments [$\sim$1000 Å diameter (*32*, *33*)], phosphorus NMR measurements suggest that the outer leaflet has about 4% more lipid than the outer one (*47*). This will also increase the equilibrium T-value. For these reasons, it is not unreasonable to expect T to be 0.55−0.60 for TOA and TOE. The same reasoning probably explains why the T-values for the amphipathic peptides are, on average, slightly greater than 1.0.

Topology of Amphipathic Helices. The peptides Ac-18A-NH_2, Ac-8A1-NH_2, Ac-18A2-NH_2, and Ac-18AY-NH_2 examined in our experiments are models for the amphipathic helices of apolipoprotein A−I (*48*, *49*). They are all highly charged peptides and are strongly helical in bilayer interfaces (*48*, *49*), where they lie parallel to the bilayer surface (*50*). At concentrations of $\sim$0.5 mol %, none them caused flip-flop of lysoMC and all had $T \sim 1$ (Table 1), unequivocally localizing them on the outer monolayer of the vesicles. This result did not change after as much as 24 h of incubation. As discussed elsewhere in detail (*2*), the absolute free energy of transfer of a peptide into lipid bilayers as determined by partition coefficient measurements depends on whether the peptide has free access to both bilayer leaflets. If a peptide has access to only one leaflet, then the effective lipid concentration for partitioning is one-half the total concentration. This results in a lowering of the computed free energy of transfer by 0.4 kcal mol^{-1} (*2*), i.e., stronger effective partitioning. Our lysoMC−RET method offers the possibility of determining the inner bilayer accessibility in many cases.

Melittin, the principal toxic component of honey bee venom, is well-known to form transmembrane pores across some bilayers under appropriate conditions (*51*, *52*). Unfortunately, our lysoMC−RET method cannot be used for the determination of melittin topology in POPC vesicles because it induces rapid transbilayer equilibration of lysoMC at concentrations as low as 0.1 mol % (Figure 6). This may, of course, be an indirect indication that melittin at least transiently crosses the bilayer, as implied by other experiments (*12*, *35*, *52*−*55*). In this light, it is interesting that 0.5 mol % melittin does not induce lysoMC flip-flop nor does it transit the bilayer to the inner leaflet in POPG vesicles ($T \sim 1$), consistent with the observation that melittin does not form sizable pores in POPG vesicles (Ladokhin, A. S., and White, S. H., unpublished observation). This is in sharp contrast to POPC vesicles in which melittin forms very large pores (*54*).

These results show the usefulness of the lysoMC−RET method for exploring the interactions of peptides with membranes, especially in conjunction with other types of measurements. It is easily implemented and gives, in many cases, an unambiguous description of a Trp-containing molecule's topology in lipid bilayers.

ACKNOWLEDGMENT

We thank Drs. Kalina Hristova and Alexey Ladokhin for many helpful discussions, and Drs. Vinod Mishra and Jere Segrest for their kind gift of the Ac-18A-NH_2 amphipathic peptides. We thank an unknown referee for his/her detailed comments and suggestions regarding the treatment of RET on membranes.

REFERENCES

1. White, S. H., and Wimley, W. C. (1994) *Curr. Opin. Struct. Biol. 4*, 79−86.
2. White, S. H., Wimley, W. C., Ladokhin, A. S., and Hristova, K. (1998) *Methods Enzymol. 295*, 62−87.
3. White, S. H., and Wimley, W. C. (1998) *Biochim. Biophys. Acta 1376*, 339−352.
4. White, S. H., and Wimley, W. C. (1999) *Annu. Rev. Biophys. Biomol. Struct. 28*, 319−365.
5. He, K., Ludtke, S. J., Huang, H. W., and Worcester, D. L. (1995) *Biochemistry 34*, 15614−15618.
6. Lambotte, S., Jasperse, P., and Bechinger, B. (1998) *Biochemistry 37*, 16−22.
7. Axelsen, P. H., and Citra, M. J. (1997) *Prog. Biophys. Mol. Biol. 66*, 227−253.
8. Gray, C., and Tamm, L. K. (1997) *Protein Sci. 6*, 1993−2006.
9. Wu, Y., Huang, H. W., and Olah, G. A. (1990) *Biophys. J. 57*, 797−806.
10. Ramaswami, V., Zhu, X. Y., Romanowski, M., Haaseth, R. C., Misicka, A., Lipkowski, A. W., Hruby, V. J., and O'Brien, D. F. (1996) *Int. J. Pept. Protein Res. 48*, 87−94.
11. Maduke, M. and Roise, D. (1993) *Science 260*, 364−367.
12. Matsuzaki, K., Murase, O., Fujii, N., and Miyajima, K. (1995) *Biochemistry 34*, 6521−6526.
13. Everett, J., Zlotnick, A., Tennyson, J., and Holloway, P. W. (1986) *J. Biol. Chem. 261*, 6725−6729.
14. Stryer, L., and Haugland, R. P. (1967) *Proc. Natl. Acad. Sci. U.S.A. 58*, 719−726.
15. Lakowicz, J. R. (1983) *Principles of Fluorescence Spectroscopy*, Plenum Press, New York.
16. Wimley, W. C., and White, S. H. (1993) *Biochemistry 32*, 6307−6312.
17. Schiffer, M., Chang, C. H., and Stevens, F. J. (1992) *Protein Eng. 5*, 213-214.
18. Kachel, K., Asuncion-Punzalan, E., and London, E. (1995) *Biochemistry 34*, 15475−15479.
19. Wiener, M. C., and White, S. H. (1992) *Biophys. J. 61*, 434−447.
20. Ren, J. H., Lew, S., Wang, Z. W., and London, E. (1997) *Biochemistry 36*, 10213−10220.
21. Liu, L.-P., and Deber, C. M. (1997) *Biochemistry 36*, 5476−5482.
22. Stafford, R. E., Fanni, T., and Dennis, E. A. (1989) *Biochemistry 28*, 5113−5120.
23. de Kruijff, B., van den Besselaar, A. M. H. P., and van Deenen, L. L. M. (1977) *Biochim. Biophys. Acta 465*, 443−453.
24. Bhamidipati, S., and Hamilton, J. A. (1995) *Biochemistry 34*, 5666−5677.
25. Permyakov, E. A. (1993) *Luminescent Spectroscopy of Proteins*, CRC Press, Boca Raton.
26. Wolber, P. K., and Hudson, B. S. (1979) *Biophys. J. 28*, 197−210.
27. Davenport, L., Dale, R. E., Bisby, R. H., and Cundall, R. B. (1985) *Biochemistry 24*, 4097−4108.
28. Ladokhin, A. S., Malak, H., Johnson, M. L., Lakowicz, J. R., Wang, L., Steggles, A. W., and Holloway, P. W. (1992) in *Time-Resolved Laser Spectroscopy in Biochemistry III* (Lakowicz, J. R., Ed.) pp 1−807, SPIE, Bellingham, WA.
29. Wu, P. G., and Brand, L. (1994) *Anal. Biochem. 218*, 1−13.
30. Tatischeff, I., and Klein, R. (1975) *Photochem. Photobiol. 22*, 221−229.
31. Marsh, D. (1990) *CRC Handbook of Lipid Bilayers*, CRC Press, Boca Raton.
32. Mayer, L. D., Hope, M. J., and Cullis, P. R. (1986) *Biochim. Biophys. Acta 858*, 161−168.
33. Hope, M. J., Bally, M. B., Mayer, L. D., Janoff, A. S., and Cullis, P. R. (1986) *Chem. Phys. Lipids 40*, 89−107.
34. Zhelev, D. V. (1996) *Biophys. J. 71*, 257−273.
35. Fattal, E., Nir, S., Parente, R. A., and Szoka, F. C. (1994) *Biochemistry 33*, 6721−6731.
36. Matsuzaki, K., Murase, O., Fujii, N., and Miyajima, K. (1996) *Biochemistry 35*, 11361−11368.
37. Homan, R., and Pownall, H. J. (1988) *Biochim. Biophys. Acta 938*, 155−1667.
38. Wimley, W. C., and Thompson, T. E. (1991) *Biochemistry 30*, 1702−1709.
39. Hall, J. E. (1981) *Biophys. J. 33*, 373−381.
40. Jones, J. D., and Thompson, T. E. (1989) *Biochemistry 28*, 129−134.
41. Bolen, E. J., and Holloway, P. W. (1990) *Biochemistry 29*, 9638−9643.
42. Disalvo, E. A., and Simon, S. A. (1995) *Permeability and Stability of Lipid Bilayers*, CRC Press, Boca Raton.
43. Wimley, W. C., and White, S. H. (1996) *Nat. Struct. Biol. 3*, 842−848.
44. Yau, W.-M., Wimley, W. C., Gawrisch, K., and White, S. H. (1998) *Biochemistry 37*, 14713−14718.
45. Ladokhin, A. S., and Holloway, P. W. (1995) *Biophys. J. 69*, 506−517.
46. Ladokhin, A. S. (1997) *Methods Enzymol. 278*, 462−473.
47. Hope, M. J., Bally, M. B., Webb, G., and Cullis, P. R. (1985) *Biochim. Biophys. Acta 812*, 55−65.
48. Venkatachalapathi, Y. V., Phillips, M. C., Epand, R. M., Epand, R. F., Tytler, E. M., Segrest, J. P., and Anantharamaiah, G. M. (1993) *Proteins 15*, 349−359.
49. Mishra, V. K., and Palgunachari, M. N. (1996) *Biochemistry 35*, 11210−11220.
50. Hristova, K., Wimley, W. C., Mishra, V. K., Anantharamaiah, G. M., Segrest, J. P., and White, S. H. (1999) *J. Mol. Biol. 290*, 99−117.
51. Dempsey, C. E. (1990) *Biochim. Biophys. Acta 1031*, 143−161.
52. Matsuzaki, K., Yoneyama, S., and Miyajima, K. (1997) *Biophys. J. 73*, 831−838.
53. Matsuzaki, K., Yoneyama, S., Murase, O., and Miyajima, K. (1996) *Biochemistry 35*, 8450−8456.
54. Ladokhin, A. S., Selsted, M. E., and White, S. H. (1997) *Biophys. J. 72*, 1762−1766.
55. Ladokhin, A. S., and Holloway, P. W. (1995) *Ukr. Biochem. J. 67*, 34−40.

BI991836L